CHIN. PHYS. LETT. Vol. 38, No. 10 (2021) 103701

Production of ^{87}Rb Bose–Einstein Condensate in an Asymmetric Crossed Optical Dipole Trap

Zhu Ma(马翥)[1,2†], Chengyin Han(韩成银)[1†], Xunda Jiang(江迅达)[1,2], Ruihuan Fang(方瑞环)[1,2], Yuxiang Qiu(邱宇翔)[1,2], Minhua Zhao(赵敏华)[1,2], Jiahao Huang(黄嘉豪)[1], Bo Lu(鹿博)[1*], and Chaohong Lee(李朝红)[1,2*]

[1]*Guangdong Provincial Key Laboratory of Quantum Metrology and Sensing & School of Physics and Astronomy, Sun Yat-Sen University (Zhuhai Campus), Zhuhai 519082, China*
[2]*State Key Laboratory of Optoelectronic Materials and Technologies, Sun Yat-Sen University (Guangzhou Campus), Guangzhou 510275, China*

(Received 20 August 2021; accepted 25 August 2021; published online 26 September 2021)

We report the production of ^{87}Rb Bose–Einstein condensate in an asymmetric crossed optical dipole trap (ACODT) without the need of an additional dimple laser. In our experiment, the ACODT is formed by two laser beams with different radii to achieve efficient capture and rapid evaporation of laser cooled atoms. Compared to the cooling procedure in a magnetic trap, the atoms are firstly laser cooled and then directly loaded into an ACODT without the pre-evaporative cooling process. In order to determine the optimal parameters for evaporation cooling, we optimize the power ratio of the two beams and the evaporation time to maximize the final atom number left in the ACODT. By loading about 6×10^5 laser cooled atoms in the ACODT, we obtain a pure Bose–Einstein condensate with about 1.4×10^4 atoms after 19 s evaporation. Additionally, we demonstrate that the fringe-type noises in optical density distributions can be reduced via principal component analysis, which correspondingly improves the reliability of temperature measurement.

DOI: 10.1088/0256-307X/38/10/103701

Atomic Bose–Einstein condensate (BEC) is an important and typical macroscopic quantum system of clean environment, controllable parameters and long coherence time. It provides an excellent platform to study many-body quantum physics, quantum simulation and quantum metrology.[1−9] There appear lots of significant achievements in this field,[10−28] such as exotic quantum phase transitions of ultracold atoms in optical lattices,[3,4] high precise measurement via Bose condensed atoms,[5−8] and spin-orbit coupled quantum atomic gases.[13]

There are many different experimental systems to produce atomic BEC. According to the trap potentials used for evaporative cooling, BEC apparatuses can be divided into three categories: magnetic trap systems, optical dipole trap (ODT) systems, and hybrid trap systems. The first two BECs were produced by evaporative cooling in magnetic trap systems.[29,30] Different kinds of magnetic traps have been developed, such as cloverleaf traps,[31] QUIC traps,[32,33] mini traps,[34] and atom chips.[35,36] The advantage of ODT systems over magnetic traps is spin-state independent. ODT systems can be made in flexible geometries to improve trap depth, trap volume, and trap frequency,[37] so that high elastic collision rate can be achieved and evaporative cooling process can be accelerated. ODT systems have been extended to a big family, such as all-optical crossed ODT,[38−41] and the optical surface trap.[42] Hybrid trap system combines the advantages of magnetic trap and ODT, which is usually composed of a pre-cooling process in a magnetic trap and a final evaporative cooling process in an ODT.[43,44]

In an ODT, the evaporative cooling is usually realized by lowering the trap laser power, which inevitably decreases both trap depth and trap frequency. This is indeed different from the situation in a magnetic trap where the trap frequency can remain constant during evaporation process. In an ODT with fixed trap depth, its trap frequency decreases with the beam size. As the elastic collision rate increases with the trap frequency, one may reduce the beam size to improve the evaporation efficiency. On the other hand, the total number of loaded atoms increases with the beam size and the trap depth. Therefore, to achieve both high evaporation efficiency and large total atom number, it is essential to design suitable trap frequency, trap

Supported by the Key-Area Research and Development Program of Guangdong Province, China (Grant No. 2019B030330001), the National Natural Science Foundation of China (Grant Nos. 12025509 and 11874434), the Science and Technology Program of Guangzhou, China (Grant Nos. 201904020024 and 201804010497), the Natural Science Foundation of Guangdong Province, China (Grant No. 2018A030313988), and the Fundamental Research Funds for the Central Universities (Grant No. 2021qntd28).
†These authors contributed equally to this work.
*Corresponding authors. Email: lubo3@mail.sysu.edu.cn; lichaoh2@mail.sysu.edu.cn

depth and beam size. Several techniques have been developed to dynamically control the ODT shape for increasing elastic collision rate and accelerating evaporative cooling, such as a zoom lens, an extra dimple laser beam, and a magnetic field gradient.[39,43–49] These methods usually require delicate optical or magnetic alignment and manipulation, which increases the experimental complexity.

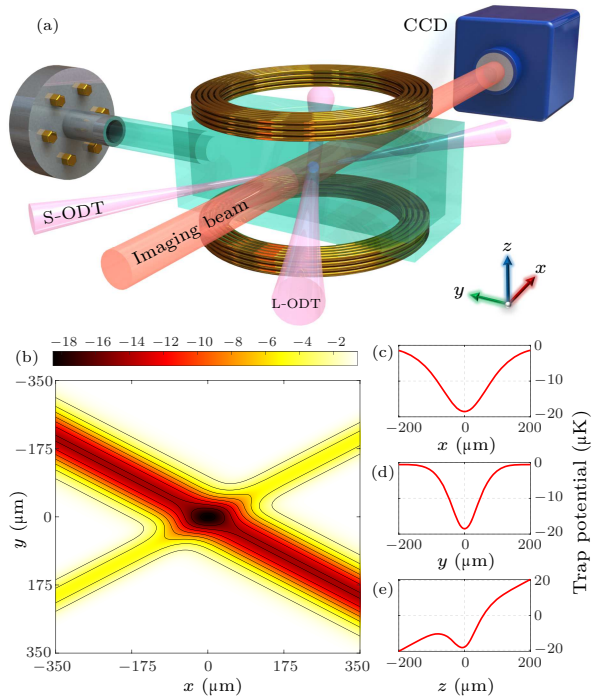

Fig. 1. (a) Schematic of our experimental setup. The anti-Helmholtz coils are in bronze. The crossed ODT beams focused by lenses are shown in pink, where S-ODT and L-ODT are separated at angles of $-30°$ and $30°$ with respect to x-axis. An imaging beam in orange is along the x-axis. (b) The contour map is plotted in xy plane at $z = z_{\min}$, $z_{\min}$ is the position of trap potential minimum along z axis. L-ODT power of 1 W and S-ODT power of 0.1 W are used for simulation. In the trap center, the region around $100 \times 100\,\mu\text{m}^2$ can form a conservative well. The trap potentials are shown along (c) x-axis, (d) y-axis, (e) z-axis.

In this Letter, we report the creation of a BEC of ^{87}Rb atoms in an asymmetric crossed optical dipole trap (ACODT). The ACODT consists of two focused laser beams intersecting at an angle of 60° with different radii to balance trap frequency and trap volume, as shown in Fig. 1. The large size beam with 82 μm radius is called large optical dipole trap (L-ODT), and the small size beam with 48 μm radius is called small optical dipole trap (S-ODT). L-ODT can trap plentiful atoms initially. S-ODT can provide high trap frequency during the evaporation process. Starting from a regular magneto-optical trap (MOT), we apply a temporal dark MOT to increase the atom density and then directly load atoms into the ACODT. We perform the evaporative cooling by optimizing both the power ratio η_i of L-ODT to S-ODT and the evaporation time τ_i to maintain the maximum atom number at the i-th evaporation step. From around 6×10^5 laser-cooled atoms loaded into the ACODT, we obtain an ^{87}Rb BEC with about 1.4×10^4 atoms after the evaporative cooling.

In our experiment, the BEC apparatus mainly consists of two glass chambers with antireflection coating from 700 nm to 1100 nm. One chamber is $45 \times 45 \times 120\,\text{mm}^3$, which is used for the first-stage three-dimensional magneto-optical trap (3D MOT). The vacuum pressure of the first chamber is about 1×10^{-7} Pa. The other chamber is $35 \times 35 \times 110\,\text{mm}^3$, which is used for the second-stage 3D MOT. The vacuum pressure of the second chamber is about 3×10^{-9} Pa. A differential tube is used to maintain the pressure difference between two chambers. The ultrahigh vacuum can ensure long lifetime of trapped atoms.

Collecting sufficient amount of laser-cooled atoms is essential for implementing evaporative cooling and producing a BEC. The first-stage 3D MOT is used for pre-cooling atoms and then the atoms are transported to the second-stage 3D MOT by a push beam. For the first-stage 3D MOT, the optimized magnetic gradient is 5 G/cm, the total intensity of cooling laser is $54\,\text{mW/cm}^2$, and the total intensity of repump laser is $6\,\text{mW/cm}^2$. The second-stage 3D MOT shares the same acousto-optic modulators (AOMs) as the first-stage 3D MOT. The optimized detunings for cooling laser and repump laser are 20 MHz below the transition $|5S_{1/2}, F = 2\rangle$ to $|5P_{3/2}, F' = 3\rangle$ and 2 MHz below the transition $|5S_{1/2}, F = 1\rangle$ to $|5P_{3/2}, F' = 2\rangle$, respectively. The first-stage 3D MOT can capture about 1×10^9 atoms within 5 s. The push beam transports atoms between two chambers through the differential tube, which is y-axis direction in our laboratory reference frame. We focus the push beam on the first-stage MOT to increase the atomic flux. The optimized push laser power is 0.8 mW and laser detuning is 35 MHz below the transition between $|5S_{1/2}, F = 2\rangle$ to $|5P_{3/2}, F' = 3\rangle$. For the second-stage MOT, by setting the magnetic gradient to 10 G/cm, the total cooling laser intensity is $39\,\text{mW/cm}^2$ and the repump laser intensity is $8\,\text{mW/cm}^2$, typically 1×10^8 atoms can be captured.

In order to increase the atoms loaded into the ACODT, the atoms must be laser cooled with high density and low temperature before loading. However the MOT density is governed by the reabsorption of scattered light in the cloud.[50,51] Performing dark MOT or temporal dark MOT is a usual method to get over the issue.[45,52] In our experiment, we initially compress the second-stage MOT by increasing the detuning of cooling laser from -20 MHz to -38 MHz and decreasing the intensity of cooling laser from $39\,\text{mW/cm}^2$ to $20\,\text{mW/cm}^2$ within 100 ms. Then

we keep the cooling laser detuning and intensity, and decrease the repump laser intensity from $8\,\mathrm{mW/cm^2}$ to $0.5\,\mathrm{mW/cm^2}$ for 5 ms to generate temporal dark MOT. In this way, the atomic density is increased to $1\times10^{12}\,\mathrm{cm^{-3}}$.

After applying the temporal dark MOT, a polarization gradient cooling (PGC) is imposed to reduce the temperature of atomic cloud. Concretely, the magnetic field is turned off immediately, the detuning of the cooling laser is further increased from -38 MHz to -55 MHz and its intensity is further decreased from $20\,\mathrm{mW/cm^2}$ to $12\,\mathrm{mW/cm^2}$ for 10 ms. The temperature after the PGC is about 30 μK. Then, the repump laser is tuned off and the cooling laser is kept on for 2 ms to pump atoms into the $|5S_{1/2}, F=1\rangle$ state which has a longer lifetime than the $|5S_{1/2}, F=2\rangle$ state in the ODT.

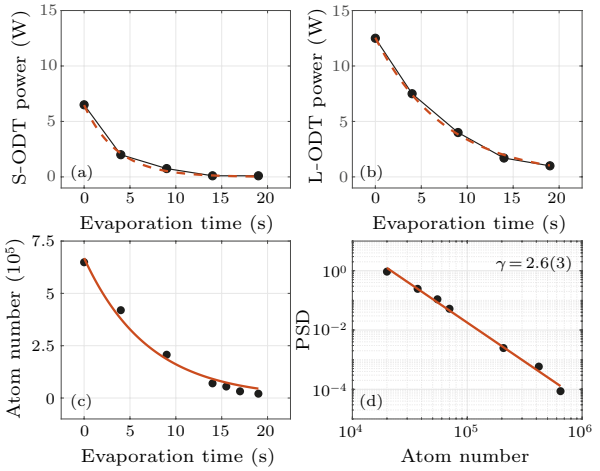

Fig. 2. Performance of evaporative cooling in an ACODT. The laser power of (a) S-ODT and (b) L-ODT versus the evaporation time. The black solid lines are obtained using the optimization method. The red dashed lines show the exponential fittings. (c) The total number of atoms left in the ACODT versus the evaporation time. (d) The PSD versus the total atom number.

The ACODT is composed of two linearly polarized laser beams, which are generated from a single mode 1064 nm fiber laser. In order to avoid the interference effects, the polarizations of two beams are orthogonal and the frequency of two beams is separated 220 MHz using two AOMs. The ACODT is turned on at the beginning of the PGC. The initial powers of L-ODT and S-ODT are 12.5 W and 6.5 W, respectively. About 6×10^5 atoms can be captured in the crossed region.

Evaporative cooling is an important process to produce an atomic BEC. Before evaporation starts, the atoms are held in the ACODT for 500 ms to reach thermal equilibrium. We separate the whole evaporation process into four steps. In each step, we linearly decrease the ACODT laser power to half the initial value. Then we optimize the power ratio η_i of L-ODT to S-ODT to maximize the atom number left in the ACODT at the end of the i-th evaporation step, where the trial evaporation time τ_i is chosen to be equal to the previous optimized evaporation time, i.e., $\tau_i = \tau_{i-1}$, $\tau_1 = \tau_\mathrm{a}/2$. Here, τ_a is the lifetime of atoms in the ACODT, which is measured before evaporation starts. In our experiment, τ_a is about 9 s. After that, we optimize the evaporation time τ_i to maximize the atom number in the ACODT by fixing the power ratio η_i. The optimized polylines are shown in Figs. 2(a) and 2(b), which are well consistent to the optimal evaporation curves as an exponential decay function. At the end of the fourth step, we obtain a pure BEC by setting the S-ODT power 0.1 W and the L-ODT power 1 W, which corresponds to a trap frequency $2\pi\times(79, 182, 166)$ Hz. The temperature and the atom number in the evaporation process are extracted via time-of-flight (TOF) absorption imaging. The atom number and phase space density (PSD) in the evaporation process are shown in Figs. 2(c) and 2(d).

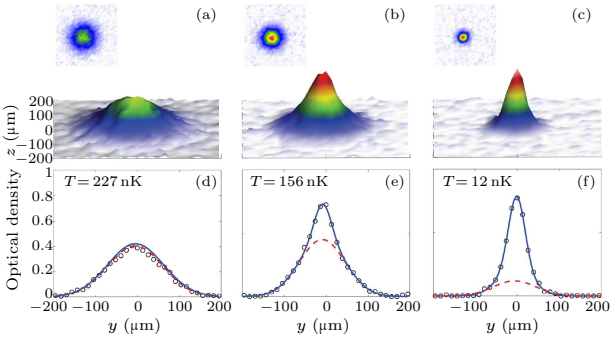

Fig. 3. Absorption images for different evaporation procedures. (a) Thermal gas, (b) mixed thermal and condensate gas, (c) pure BEC. The one-dimensional cross sections (black circles) in (d)–(f) were extracted from (a)–(c) along y-axis through the maximum of the two-dimensional absorption images. The red dash curves are Gaussian fittings of the thermal tails of atomic clouds, and the blue curves are two Gaussian functions fittings of the whole atomic clouds.

In our experiment, the evaporation efficiency $\gamma = -\log(\mathrm{PSD_f}/\mathrm{PSD_i})/\log(N_\mathrm{f}/N_\mathrm{i})$ is about 2.6(3). Before the appearance of BEC, there is only a thermal gas obeying the Boltzmann distribution, as shown in Figs. 3(a) and 3(d). By decreasing the power of ACODT, the typical bimode distribution is observed, as shown in Figs. 3(b) and 3(e), and finally there appears a pure BEC obeying the Bose–Einstein distribution, as shown in Figs. 3(c) and 3(f). By fitting multiple absorption images at different TOF times with two Gaussian functions, the temperature can be determined. At the thermal gas stage, the temperature and the atom number are 227 nK and 5.5×10^4; at the bimode stage, the temperature and the atom number are 156 nK and 2.7×10^4; at the pure BEC stage, the temperature and the atom number are 12 nK and 1.4×10^4. In our experiment, the BEC transition temperature is about 166 nK. Based upon our optimized

evaporation procedure, we create a BEC with 1.4×10^4 atoms from 6×10^5 laser-cooled atoms with a temperature of 12 μK.

In a conventional absorption imaging process, three pictures are taken in one cycle: an image of atomic cloud A, an image of light distribution L, and an image of background signal B. From these three pictures, the optical density in the yz-plane is given as

$$\mathrm{OD}(y,z) = -\ln\frac{A(y,z)-B(y,z)}{L(y,z)-B(y,z)}. \tag{1}$$

Actually, the difference between A and L is not only caused by the absorption of atomic cloud. The perturbation of light intensity as well as the vibration of the imaging system also leads to a difference between A and L, which brings an unexpected fringe-type noise in $\mathrm{OD}(y,z)$. These unexpected fringes will influence the quality of TOF absorption imaging, especially when the atom number is small.

In order to reduce the unexpected fringes, an efficient technique is to construct an ideal light distribution $\Lambda(y,z)$ from $A(y,z)$ via principal component analysis (PCA).[53] We collect a large number of light distribution images, 245 in our experiment, $\{L_m(y,z)|m\in\mathbb{N},\ 0<m\leq 245\}$. The relative light distribution is given as $\tilde{L}_m(y,z) = L_m(y,z)-B_m(y,z)-\bar{L}_m$ with $\bar{L}_m$ denoting the mean of $L_m(y,z)-B_m(y,z)$, and $B_m(y,z)$ being the background signal. Pixels of each relative light distribution $\tilde{L}_m(y,z)$ in a ring area, with internal radius r_{in} and external radius r_{ex}, are mapped into a vector $\tilde{L}^h_m$. For convenience, we use the Einstein summation convention in our following formula. Given the image of an atomic cloud $A(y,z)$ with a background signal $B(y,z)$, the relative atomic cloud distribution is $\tilde{A}(y,z) = A(y,z)-B(y,z)-\bar{A}$. Here, $\bar{A}$ is the mean of the ring area of $A(y,z)-B(y,z)$ excluding the atoms. Similarly, we map the ring area of $\tilde{A}(y,z)$ into a vector $\tilde{A}^h$.

Then one can calculate the covariance matrix $S^n_m = (\tilde{L}^T)^n_h\tilde{L}^h_m$. Through implementing the singular value decomposition, we can obtain a matrix V^m_j satisfying

$$(V^T)^i_n S^n_m V^m_j = \delta^i_j, \tag{2}$$

with the Kronecker delta notation δ. The matrix V^m_j is constructed with a set of vectors $\boldsymbol{v}_j$, and $\boldsymbol{v}_j$ is the eigenvectors of S^n_m for its top-J eigenvalues. Finally, the ideal light distribution can be reconstructed via the top-J components,

$$\Lambda(y,z) = \tilde{L}_m(y,z)V^m_j(V^T)^j_n(\tilde{L}^T)^n_h\tilde{A}^h + B(y,z) + \bar{A}. \tag{3}$$

In our experiment, we choose the internal radius $r_{\mathrm{in}} = 364\,\mu\mathrm{m}$ (which is much larger than the radius of atomic cloud), the optimal external radius $r_{\mathrm{ex}} = 1040\,\mu\mathrm{m}$ via minimizing noise signal and the number of top eigenvectors $J = 50$. Released from the ACODT trap ($P_{\text{L-ODT}} = 1.28\,\mathrm{W}$, $P_{\text{S-ODT}} = 0.1\,\mathrm{W}$), the absorption images taken after a 20 ms TOF without and with PCA are shown in Figs. 4(a) and 4(b). The fringe-type noises are effectively reduced with PCA. The temperatures extracted from TOF absorption images with and without PCA are shown in Fig. 4(c) for different ACODT powers. It is clearly seen that the temperatures extracted via PCA has a much smaller standard deviation than that of the conventional method. This means that, when fitting physical quantities such as temperature, one can obtain a reliable result if the PCA is applied to the absorption images.

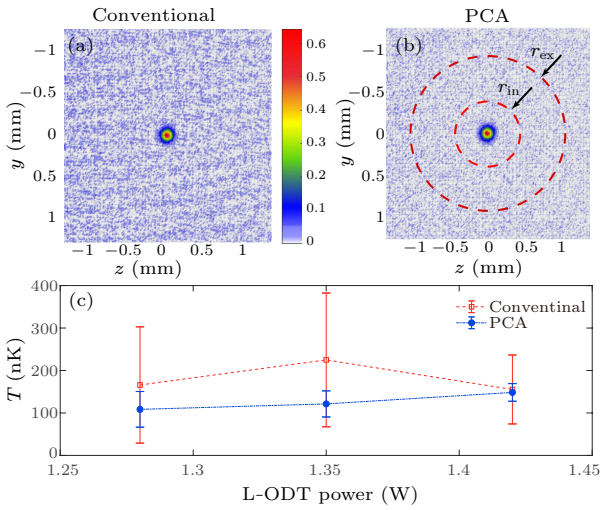

Fig. 4. Comparison of the TOF images obtained from the conventional calculation (a) and the principle component analysis (b). (c) Temperatures corresponding to different L-ODT powers with (blue circles) and without (red rectangles) the PCA. Here, the S-ODT power is fixed at 0.1 W. The error bars represent the standard deviations of five measurements.

In summary, we have demonstrated a scheme to create ^{87}Rb BEC in an ACODT without the need of an additional dimple laser. The ACODT is formed by two crossed laser beams with different radii to balance trap frequency and trap volume. In contrast to the cooling procedure in a magnetic trap, which needs a pre-evaporative cooling process, our scheme firstly cools the atoms with lasers and then directly loads them into an ACODT for implementing evaporative cooling. To maximize the final atom number, we implement the evaporative cooling by optimizing both the power ratio between two asymmetric beams and the evaporation time. Our strategy to determine the optimal parameters during evaporation process is simple and efficient. Even with relatively small initial atom numbers, in our case, only 6×10^5 laser-cooled ^{87}Rb atoms loaded into the ACODT, we have successfully observed the BEC phase transition and obtained a pure BEC with 1.4×10^4 atoms. Our scheme is not

specific to ^{87}Rb and can be applied to achieve optimal evaporative efficiency for other atomic species that is evaporatively cooled in optical traps. Additionally, we obtain a more reliable temperature measurement of atomic cloud through implementing PCA of TOF absorption images.

References

[1] Greiner M, Mandel O, Esslinger T, Hänsch T W and Bloch I 2002 *Nature* **415** 39
[2] Léonard J, Morales A, Zupancic P, Donner T and Esslinger T 2017 *Science* **358** 1415
[3] Clark L W, Feng L and Chin C 2016 *Science* **354** 606
[4] Braun S, Friesdorf M, Hodgman S S, Schreiber M, Ronzheimer J P, Riera A, del Rey M, Bloch I, Eisert J and Schneider U 2015 *Proc. Natl. Acad. Sci. USA* **112** 3641
[5] Lee C H, Huang J H, Deng H M, Dai H and Xu J 2012 *Front. Phys.* **7** 109
[6] Gross C, Zibold T, Nicklas E, Estève J and Oberthaler M K 2010 *Nature* **464** 1165
[7] Lee C H 2006 *Phys. Rev. Lett.* **97** 150402
[8] SøR A, Duan L M, Cirac J I and Zoller P 2001 *Nature* **409** 63
[9] Léonard J, Morales A, Zupancic P, Esslinger T and Donner T 2017 *Nature* **543** 87
[10] Ji S C, Zhang J Y, Zhang L, Du Z D, Zheng W, Deng Y J, Zhai H, Chen S and Pan J W 2014 *Nat. Phys.* **10** 314
[11] Dai H N, Yang B, Reingruber A, Xu X F, Jiang X, Chen Y A, Yuan Z S and Pan J W 2016 *Nat. Phys.* **12** 783
[12] Yang B, Chen Y Y, Zheng Y G, Sun H, Dai H N, Guan X W, Yuan Z S and Pan J W 2017 *Phys. Rev. Lett.* **119** 165701
[13] Wu Z, Zhang L, Sun W, Xu X T, Wang B Z, Ji S C, Deng Y J, Chen S, Liu X J and Pan J W 2016 *Science* **354** 83
[14] Peng P, Huang L H, Li D H, Wang P J, Meng Z M, Zhang J 2018 *Chin. Phys. Lett.* **35** 063201
[15] Nawaz K S, Mi C D, Chen L C, Wang P J and Zhang J 2019 *Chin. Phys. Lett.* **36** 043201
[16] Chen L C, Wang P J, Meng Z M, Huang L H, Cai H, Wang D W, Zhu S Y and Zhang J 2018 *Phys. Rev. Lett.* **120** 193601
[17] Yang S F, Xu Z T, Wang K, Li X F, Zhai Y Y and Chen X Z 2019 *Chin. Phys. Lett.* **36** 080302
[18] Yang S F, Zhou T W, Li C, Yang K X, Zhai Y Y, Yue X G and Chen X Z 2020 *Chin. Phys. Lett.* **37** 040301
[19] Chen S, Zhou X J, Yang F, Xia L, Wang Y Q and Chen X Z 2004 *Chin. Phys. Lett.* **21** 2227
[20] Tang P J, Peng P, Li Z H, Chen X Z, Li X P and Zhou X J 2019 *Phys. Rev. A* **100** 013618
[21] Deng L, Hagley E W, Cao Q, Wang X R, Luo X Y, Wang R Q, Payne M G, Yang F, Zhou X J, Chen X Z and Zhan M S 2010 *Phys. Rev. Lett.* **105** 220404
[22] Zhang D F, Gao T Y, Zou P, Kong L R, Li R Z, Shen X, Chen X L, Peng S G, Zhan M S, Pu H and Jiang K J 2019 *Phys. Rev. Lett.* **122** 110402
[23] Deng S J, Shi Z Y, Diao P P, Yu Q L, Zhai H, Qi R and Wu H B 2016 *Science* **353** 371
[24] Li B, Jiang X J, Li X L, Hai W H and Wang Y Z 2019 *Chin. Phys. B* **28** 100303
[25] Hu Z F, Liu C P, Liu J M and Wang Y Z 2018 *Opt. Express* **26** 20122
[26] Gao K Y, Luo X Y, Jia F D, Yu C H, Zhang F, Yin J P, Xu L, You L and Wang R Q 2014 *Chin. Phys. Lett.* **31** 063701
[27] Luo X Y, Zou Y Q, Wu L N, Liu Q, Han M F, Tey M K and You L 2017 *Science* **355** 620
[28] Qiu L Y, Liang H Y, Yang Y B, Yang H X, Tian T, Xu Y and Duan L M 2020 *Sci. Adv.* **6** eaba7292
[29] Anderson M H, Ensher J R, Matthews M R, Wieman C E and Cornell E A 1995 *Science* **269** 198
[30] Davis K B, Mewes M O, Andrews M R, van Druten N J, Durfee D S, Kurn D M and Ketterle W 1995 *Phys. Rev. Lett.* **75** 3969
[31] Mewes M O, Andrews M R, van Druten N J, Kurn D M, Durfee D S and Ketterle W 1996 *Phys. Rev. Lett.* **77** 416
[32] Esslinger T, Bloch I and Hänsch T W 1998 *Phys. Rev. A* **58** R2664
[33] Wang Y Z, Zhou S Y, Long Q, Zhou S Y and Fu H X 2003 *Chin. Phys. Lett.* **20** 799
[34] Wang R Q, Liu M C, Minardi F and Kasevich M 2007 *Phys. Rev. A* **75** 013610
[35] Yan B, Cheng F, Ke M, Li X L, Tang J Y and Wang Y Z 2009 *Chin. Phys. B* **18** 4259
[36] Fortagh J, Grossmann A, Zimmermann C and Hänsch T W 1998 *Phys. Rev. Lett.* **81** 5310
[37] Grimm R, Weidemüller M and Ovchinnikov Y B 2000 *Adv. At. Mol. Opt. Phys.* **42** 95
[38] Barrett M D, Sauer J A and Chapman M S 2001 *Phys. Rev. Lett.* **87** 010404
[39] Weber T, Herbig J, Mark M, Nägerl H C and Grimm R 2003 *Science* **299** 232
[40] Fazal R, Li J Z, Chen Z W, Qin Y, Lin Y Y, Zhang Z X, Zhang S C, Huang W, Yan H and Zhu S L 2020 *Chin. Phys. Lett.* **37** 036701
[41] Rychtarik D, Engeser B, Nägerl H C and Grimm R 2004 *Phys. Rev. Lett.* **92** 173003
[42] Kinoshita T, Wenger T and Weiss D S 2005 *Phys. Rev. A* **71** 011602(R)
[43] Lin Y J, Perry A R, Compton R L, Spielman I B and Porto J V 2009 *Phys. Rev. A* **79** 063631
[44] Duan Y F, Jiang B N, Sun J F, Liu K K, Xu Z and Wang Y Z 2013 *Chin. Phys. B* **22** 056701
[45] Xie D Z, Wang D Y, Gou W, Bu W H and Yan B 2018 *J. Opt. Soc. Am. B* **35** 500
[46] Hung C L, Zhang X B, Gemelke N and Chin C 2008 *Phys. Rev. A* **78** 011604(R)
[47] Huang C Y, Chen C C, Sun L A, Liao G B, Wu K S, Lin Y J and Chang M S 2017 *J. Phys. B: At. Mol. Opt. Phys.* **50** 155302
[48] Jacob D, Mimoun E, De Sarlo L, Weitz M, Dalibard J and Gerbier F 2011 *New J. Phys.* **13** 065022
[49] Olson A J, Niffenegger R J and Chen Y P 2013 *Phys. Rev. A* **87** 053613
[50] Zhang S C, Chen J F, Liu C, Zhou S Y, Loy M M T, Wong G K L and Du S W 2012 *Rev. Sci. Instrum.* **83** 073102
[51] Walker T, Sesko D and Wieman C 1990 *Phys. Rev. Lett.* **64** 408
[52] Townsend C G, Edwards N H, Zetie K P, Cooper C J, Rink J and Foot C J 1996 *Phys. Rev. A* **53** 1702
[53] Niu L X, Guo X X, Zhan Y, Chen X Z, Liu W M and Zhou X J 2018 *Appl. Phys. Lett.* **113** 144103